JACS
JOURNAL OF THE AMERICAN CHEMICAL SOCIETY
Communication
pubs.acs.org/JACS

Resolving Fine Structures of the Electric Double Layer of Electrochemical Interfaces in Ionic Liquids with an AFM Tip Modification Strategy

Yun-Xin Zhong, Jia-Wei Yan,* Mian-Gang Li, Xiao Zhang, Ding-Wen He, and Bing-Wei Mao*

State Key Laboratory of Physical Chemistry of Solid Surfaces and Department of Chemistry, College of Chemistry and Chemical Engineering, Xiamen University, Xiamen 361005, China

Supporting Information

ABSTRACT: We report enhanced force detection selectivity based on Coulombic interactions through AFM tip modification for probing fine structures of the electric double layer (EDL) in ionic liquids. When AFM tips anchored with alkylthiol molecular layers having end groups with different charge states (e.g., $-CH_3$, $-COO^-$, and $-NH_3^+$) are employed, Coulombic interactions between the tip and a specified layering structure are intensified or diminished depending on the polarities of the tip and the layering species. Systematic potential-dependent measurements of force curves with careful inspection of layered features and thickness analysis allows the fine structure of the EDL at the Au(111)−$OMIPF_6$ interface to be resolved at the subionic level. The enhanced force detection selectivity provides a basis for thoroughly understanding the EDL in ionic liquids.

Room-temperature ionic liquids (ILs) are composed of asymmetric organic cations and multiatom inorganic or organic anions and exhibit important features such as wide electrochemical windows, good conductivity, thermal stability, and many other designable properties. However, the asymmetric structures of large organic cations and the high ionic strength make ILs anisotropic media with strong interactions, so the electrochemical interfaces in ILs have distinct structures.[1,2] Resolving the fine structure of the electric double layer (EDL) in an IL is vitally important for constituting a clear physical picture about the interface. A number of theoretical studies have been devoted to understanding the structure and dynamics of electrified interfaces in ILs.[1,3,4] It has been suggested[1,3c] that the ions of ILs may overscreen the surface charges or reach lattice saturation depending on the surface charge density, which leads to a multilayer arrangement of IL ions in the EDL. Relevant experimental investigations have been carried out to reveal details of surface lateral structures and interactions[2d,5−8] as well as structures normal to surfaces.[9−13] Especially, force-sensitive techniques such as atomic force microscopy (AFM)-based force spectroscopy,[10−12] frequency-modulation AFM,[7] and surface force apparatus[13] (SFA) have become important means for probing layered structures of ILs at electrochemical interfaces.

However, layered structures exist in the entire region of an electrode−IL interface, including the region that is outside the EDL region, and the entities in the layered structures are not fixed either. To elucidate the EDL structures in ILs, two-fold efforts are necessary. First, systematic potential-dependent measurements of layered structures need to be carried out across the potential of zero charge (PZC) to bring out information associated with the EDL. On the basis of this strategy, we have revealed in our previous work the existence of charged interior layers and neutral exterior layers at the interface of Au(111) with the IL 1-butyl-3-methylimidazolium hexafluorophosphate ($BMIPF_6$).[11a] Second, the layered structures should be resolved down to ionic identity and even at the submolecular level. The group of Atkin reported the observation of a single ionic layered structure on the force curve, but the statistics of the measurements were not shown.[10d] In general, bare AFM probes are not particularly sensitive to distinguish charged layering species with different polarities.

In fact, while the sensitivity of force detection is determined by the spring constant of the cantilever of an AFM probe, the selectivity relies on both the sensitivity and specific interactions of the AFM tip with a layered structure. In this work, we employed a tip modification strategy to intensify the interaction between the tip and a specific layered structure, allowing cations, anions, and even neutral or charged parts of the cation to be resolved with high probability. It is worth mentioning that an AFM tip modified with a negatively charged silica sphere has been used to probe long-range electrostatic forces created between the charged silica sphere and ionic species in aqueous solutions.[14] However, such an approach is not applicable to probe the EDL in ILs, which is as compact as a few molecular layers with layered structure having very small rupture forces (several nN).

As illustrated in Figure 1, AFM tip modification in this work was achieved by anchoring alkylthiol molecular layers with end groups such as $-CH_3$, $-COO^-$, and $-NH_3^+$. Compared with a bare tip, modifying the tip with negatively charged end groups would increase the repulsive forces when a negatively charged anion region of a layered structure is encountered (Figure 1B), resulting in increased upward bending of the cantilever and an enlargement of the sawtooth force transitions on the force−distance curves. In contrast, modifying the tip with positively charged end groups (Figure 1C) would increase the attractive forces when the same anion part is encountered, resulting in increased downward bending of the cantilever and a reduction of the sawtooth force transitions. Opposite situations would occur

Received: August 11, 2014
Published: October 7, 2014

   dx.doi.org/10.1021/ja508222m | J. Am. Chem. Soc. 2014, 136, 14682−14685

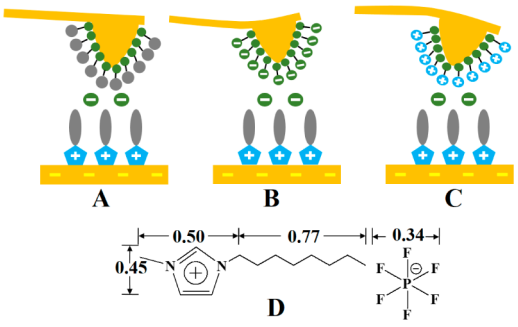

Figure 1. (A–C) Schematic illustration of the tip modification strategy using (A) neutral, (B) negatively charged, or (C) positively charged end groups. (D) Molecular structure of $OMIPF_6$. Lengths in nanometers are shown.

when modified tips encounter positively charged cation regions. Therefore, the introduction of repulsive/attractive forces enhances/reduces the sensitivity and selectivity toward the corresponding layered structure.

Au(111) in the IL 1-octyl-3-methylimidazolium hexafluorophosphate ($OMIPF_6$) has a potential of zero charge (PZC) of −0.76 V vs Pt wire, as measured using the immersion method[15] (Figure S1 in the Supporting Information). In the measurement, the current flow upon contact of a dry Au(111) surface with the IL under potential control was recorded. With the assumption of zero charge in the dried state, the corresponding charge flux is regarded as the surface charge at the specified potential. From a fit of the obtained q–E curve, the PZC of the system is determined as the potential where the charge flux is zero.

Force curves obtained using bare and modified tips are shown in Figure 2. The force–distance curve recorded using the bare tip

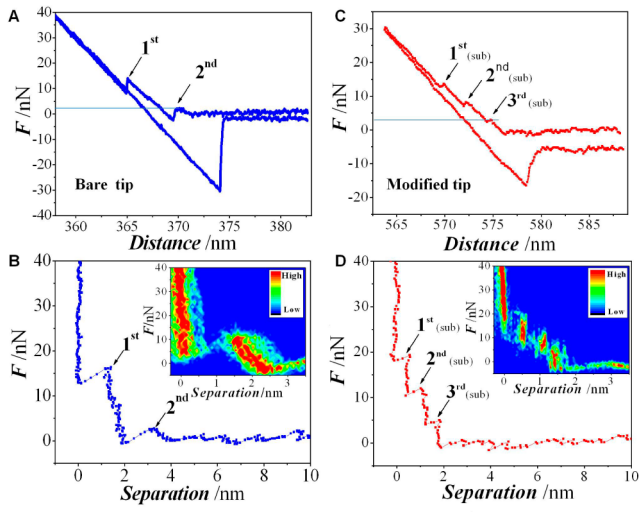

Figure 2. (A, C) Typical force–distance curves recorded at −1.4 V with (A) a bare tip and (C) a tip modified with a neutral end group. (B, D) Force–separation curves for (A) and (C), respectively. 2D histograms of 30 consecutively measured force curves are given as insets.

(Figure 2A) shows two sawtooth transitions with rupture forces of 15.3 and 2 nN for the first and second layered structures from the surface, respectively. The corresponding layer thicknesses are 1.38 and 1.32 nm, respectively, which match the size of a whole $OMIPF_6$ molecule. Our previous potential-dependent investigations on the Au(111)–$OMIPF_6$ interface using bare tips disclosed that only the first layer is charged over a wide potential range, so the EDL of this system is only one layer thick.[11b] For tips modified with a neutral end group, three sawtooth transitions are present (Figure 2C). However, the thickness is reduced to 0.51, 0.58, and 0.31 nm from the first to the third transition, respectively. These thickness values are much smaller than the molecular size and just consistent with the sizes of the imidazolium ring, octyl chain, and anion part of an $OMIPF_6$ molecule (Figure 1D), respectively, and we call such layers "sublayers" to distinguish them from the layer for the whole $OMIPF_6$ molecule. The probability of sublayer detection with the modified tip is around 30%. This is much higher than the probability of 2% that is occasionally achieved using bare tips, implying that the presence of a molecular layer on the tip does not degrade the overall quality of the AFM probe. However, we mention that the modified tip seems to be insensitive to the neutral second layer, signaling a difference from bare tips.

The force–distance curves were converted to force–separation curves[12a] to facilitate direct estimation of the thickness and inspection of the rigidity of the layered structure. On the force–separation curve recorded using bare tips (Figure 2B), the force transitions associated with the $OMIPF_6$ layered structure appear sloped, indicating insufficient rigidity of the molecular layered structure. However, the force transitions become almost vertical when the sublayer structures are resolved using the modified tip (Figure 2D), meaning that the apparent sloped force transitions of the $OMIPF_6$ layered structure may arise from relative movement of different parts of the molecule. Two-dimensional force and separation histograms were constructed (Figure 2B,D insets), from which the most probable thicknesses were estimated for the sublayer structures. The results were found to be similar for the bare and modified tips.

The selectivity of tips modified with different charge states to probe the detailed interfacial structure of $OMIPF_6$ is demonstrated further at three typical potentials across the PZC. At potentials negative of the PZC (e.g., −1.4 V; Figure 3A–C), the first layer near the surface is expected to be a cation layer, which is followed by the anion layer on top of the cation layer. Typical high-quality force curves obtained using tips modified with neutral, negative, and positive end groups all show three force transitions (sublayers). The associated thicknesses are compatible with the sizes of the OMI^+ ring, octyl side chain, and PF_6^- anion, consistent with the expected arrangement of the cations and anions. However, the responses of the cantilevers of the modified probes are different for different sublayer structures. The force values of the first sublayer probed by the three kinds of modified tips are close to each other, indicating that the first sublayer is sufficiently stable that the influence of electrostatic interactions is negligibly small. The third sublayer, associated with the anion arrangement, displays the largest apparent rupture force when probed by the tip modified with the negatively charged end group (Figure 3B) and the smallest apparent rupture force when probed by the tip modified with the positively charged end group (Figure 3C). Therefore, the tip modified with the negatively charged end group is more sensitive to detect the sublayer structure at potentials negative of the PZC.

At potentials positive of the PZC (e.g., 0 V), three force transitions are also identified on all of the force curves regardless of the tip charge state (Figure 3D–F). The apparent rupture force of the third sublayer becomes the largest when probed by tips modified with positively charged end groups. The corresponding force values and thicknesses suggest that the sublayers are arranged in an order of anion, imidazolium ring, and alkyl chain from the surface, as expected. Therefore, tips modified

dx.doi.org/10.1021/ja508222m | J. Am. Chem. Soc. 2014, 136, 14682–14685

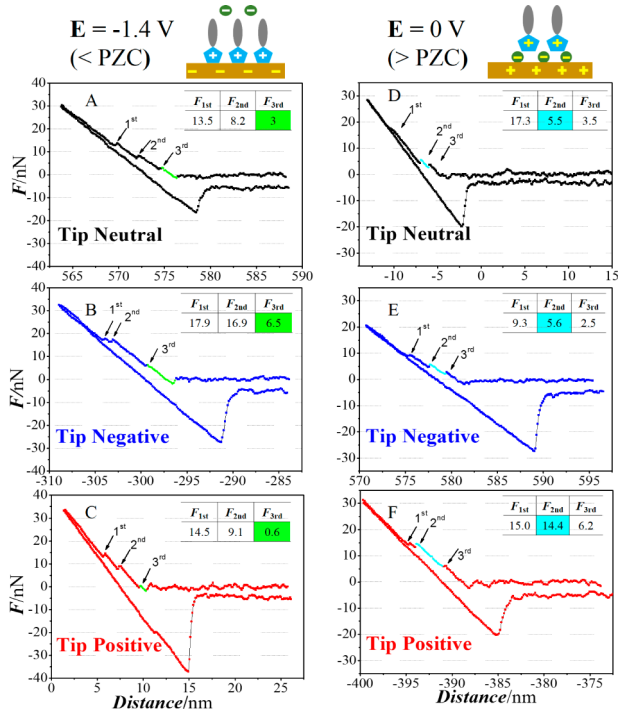

Figure 3. Typical force−distance curves at (A−C) −1.4 V and (D−F) 0 V with modified tips. The force values for the sublayers shown in the insets.

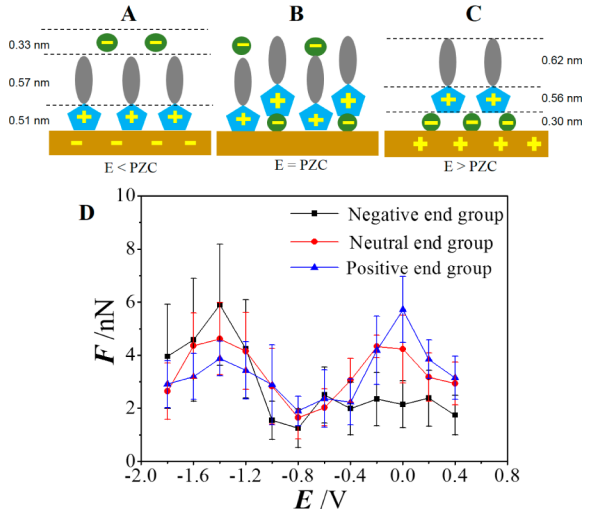

Figure 4. (A−C) Proposed arrangements of ionic entities of $OMIPF_6$ in the EDL on Au(111) surface at various potentials. (D) Potential dependence of the rupture force of the third sublayer using tips modified with different end groups.

with positively charged groups are more sensitive to detect the EDL at potentials positive of the PZC.

For potentials near the PZC, the surface is little charged, so cations and anions can have more flexible arrangements. Normally only two force transitions were detected with tips modified with any charge state (Figure S7). The rupture forces are much smaller than those at charged surfaces, implying that the stability of the sublayer structure decreases, which prevents us from distinguishing the imidazolium ring from the alkyl chain in the cation part.

As shown above, the modified tips can increase the detection selectivity toward sublayer structures without disturbing the structure of the interface, which forms the basis for probing the fine structure of the EDL. To confirm the detailed arrangement of the ionic entities in the $OMIPF_6$ molecular layered structure, accurate estimation based on statistical analysis of the thickness must be carried out. Fifty typical high-quality force curves bearing three clear force transitions were used to construct thickness histograms. A detailed analysis is presented in Figure S8 for a potential of −1.4 V. The most probable thicknesses for the first, second, and third sublayers are 0.51, 0.57, and 0.33 nm, respectively, corresponding indeed to the expected arrangement of imidazolium ring, alkyl chain, and anion of $OMIPF_6$, respectively, at −1.4 V. The thicknesses estimated using force curves with tips modified with negatively charged end groups give similar values within an error of up to 12%. Statistical analysis of the thicknesses of the sublayers at at positively charged surface was also performed (Figure S10). On the basis of the thickness analysis, possible EDLs of the Au(111)−$OMIPF_6$ interface at different surface charge states are proposed (Figure 4A−C). At negatively charged surfaces (E < PZC), the imidazolium cations are oriented with the ring toward the surface and the PF_6^- anion located at the outmost position. At positively charged surfaces (E > PZC), anions are located nearest the surface and cations are oriented with their ring toward the anion sublayer. At the PZC, a chessboard arrangement of cations and anions is speculated.

Finally, the potential dependence of the apparent rupture force of the third sublayer, which is most sensitive to the charge state of the tip, was examined with tips modified with negative, neutral, and positive charge states. It can be seen from Figure 4D that all of the force versus potential curves exhibit camel-shaped potential dependences regardless of the tip charge state, although with the negatively charged tip the increase in the force levels off at potentials more positive than the PZC because the negatively charged tip lacks a repulsive interaction with the neutral tail of the outermost alkyl chain of the cation while the attractive interaction with the positively charged imidazolium ring would diminish the apparent rupture force. On the curves showing normal camel-shaped potential dependence, the force minimum is located at around −0.8 V, which is consistent with the PZC measured by the immersion method. The two force maxima seen at −1.4 and 0.0 V correspond to the most stable structures at potentials negative and positive of the PZC, respectively, and are attributed as results of a compromise between compactness of the sublayer structure and electrostatic balance among the neighboring sublayer structures as the surface charge density increases.

To summarize, we have employed an AFM tip modification strategy based on Coulombic interactions between the tip and the charged layer to resolve the fine structure of the EDL in ILs. Potential-dependent measurements of force curves and statistical analyses of the thicknesses of the sublayer structures are important to assist detailed structural analysis of the EDL. Since the outermost layered structures in the double layer region are most sensitive to electrostatic interactions with the charged tip, modification of the tip with negatively/positively charged end groups facilitates sensitive detection of sublayer structures at potentials negative/positive of the PZC for the Au(111)−$OMIPF_6$ interface, which shines light on the complex electrode−IL interface. At the Au(111)−$OMIPF_6$ interface, the EDL at potentials negative of the PZC has a fine structure in the order of the imidazolium ring, the alkyl chain, and then the anion. The order changes to the anion, the imidazolium ring, and then the

dx.doi.org/10.1021/ja508222m | J. Am. Chem. Soc. 2014, 136, 14682−14685

alkyl chain at potentials positive of the PZC. It should be pointed out that IL species may be strongly adsorbed and immobilized on the surface depending on the potential. However, such an adsorbed layer does not obviously create the sawtooth transition on the force curve. Nevertheless, the deviation between the slopes on the forward and backward force curves in the region where the tip touches the surface might contain information on the adsorbed layer at the surface. More importantly, the adsorbed layer can be accessed and inspected with high resolution by in situ scanning tunneling microscopy (STM).[2d] Combined investigations by STM and AFM would be expected to provide the basis for a comprehensive understanding of the EDL in ILs, including lateral resolution of the layered structure.[16]

■ ASSOCIATED CONTENT

Supporting Information

Additional force curves and experimental details. This material is available free of charge via the Internet at http://pubs.acs.org.

■ AUTHOR INFORMATION

Corresponding Authors

jwyan@xmu.edu.cn
bwmao@xmu.edu.cn

Notes

The authors declare no competing financial interest.

■ ACKNOWLEDGMENTS

The authors are grateful to Prof. A. Kornyshev at Imperial College London for the inspiration to initiate the present work. This work was supported by MOST (2012CB932902) and NSFC (21033007, 20973144, and 21321062).

■ REFERENCES

(1) Kornyshev, A. A. *J. Phys. Chem. B* **2007**, *111*, 5545.

(2) (a) Fedorov, M. V.; Kornyshev, A. A. *Chem. Rev.* **2014**, *114*, 2978. (b) MacFarlane, D. R.; Pringle, J. M.; Howlett, P. C.; Forsyth, M. *Phys. Chem. Chem. Phys.* **2010**, *12*, 1659. (c) Islam, M. M.; Alam, M. T.; Okajima, T.; Ohsaka, T. *J. Phys. Chem. C* **2009**, *113*, 3386. (d) Su, Y. Z.; Fu, Y. C.; Wei, Y. M.; Yan, J. W.; Mao, B. W. *ChemPhysChem* **2010**, *11*, 2764.

(3) (a) Fedorov, M. V.; Kornyshev, A. A. *J. Phys. Chem. B* **2008**, *112*, 11868. (b) Fedorov, M. V.; Georgi, N.; Kornyshev, A. A. *Electrochem. Commun.* **2010**, *12*, 296. (c) Bazant, M. Z.; Storey, B. D.; Kornyshev, A. A. *Phys. Rev. Lett.* **2011**, *106*, No. 046102.

(4) (a) Oldham, K. B. *J. Electroanal. Chem.* **2008**, *613*, 131. (b) Lauw, Y.; Horne, M. D.; Rodopoulos, T.; Leermakers, F. A. M. *Phys. Rev. Lett.* **2009**, *103*, No. 117801. (c) Feng, G.; Zhang, J. S.; Qiao, R. *J. Phys. Chem. C* **2009**, *113*, 4549. (d) Trulsson, M.; Algotsson, J.; Forsman, J.; Woodward, C. E. *J. Phys. Chem. Lett.* **2010**, *1*, 1191.

(5) (a) Su, Y. Z.; Fu, Y. C.; Yan, J. W.; Chen, Z. B.; Mao, B. W. *Angew. Chem., Int. Ed.* **2009**, *48*, 5148. (b) Su, Y. Z.; Yan, J. W.; Li, M. G.; Xie, Z. X.; Mao, B. W.; Tian, Z. Q. *Z. Phys. Chem.* **2012**, *226*, 979. (c) Su, Y.; Yan, J.; Li, M.; Zhang, M.; Mao, B. *J. Phys. Chem. C* **2013**, *117*, 205.

(6) (a) Gnahm, M.; Müller, C.; Répánszki, R.; Pajkossy, T.; Kolb, D. M. *Phys. Chem. Chem. Phys.* **2011**, *13*, 11627. (b) Gnahm, M.; Pajkossy, T.; Kolb, D. M. *Electrochim. Acta* **2010**, *55*, 6212.

(7) Yokota, Y.; Hara, H.; Harada, T.; Imanishi, A.; Uemura, T.; Takeya, J.; Fukui, K. *Chem. Commun.* **2013**, *49*, 10596.

(8) (a) Baldelli, S. *Acc. Chem. Res.* **2008**, *41*, 421. (b) Yuan, Y. X.; Niu, T. C.; Xu, M. M.; Yao, J. L.; Gu, R. A. *J. Raman Spectrosc.* **2010**, *41*, 516.

(9) Mezger, M.; Schroder, H.; Reichert, H.; Schramm, S.; Okasinski, J. S.; Schoder, S.; Honkimaki, V.; Deutsch, M.; Ocko, B. M.; Ralston, J.; Rohwerder, M.; Stratmann, M.; Dosch, H. *Science* **2008**, *322*, 424.

(10) (a) Atkin, R.; Warr, G. G. *J. Phys. Chem. C* **2007**, *111*, 5162. (b) Hayes, R.; El Abedin, S. Z.; Atkin, R. *J. Phys. Chem. B* **2009**, *113*, 7049. (c) Hayes, R.; Borisenko, N.; Tam, M. K.; Howlett, P. C.; Endres, F.; Atkin, R. *J. Phys. Chem. C* **2011**, *115*, 6855. (d) Li, H.; Wood, R. J.; Endres, F.; Atkin, R. *J. Phys.: Condens. Matter* **2014**, *26*, No. 284115.

(11) (a) Zhang, X.; Zhong, Y. X.; Yan, J. W.; Su, Y. Z.; Zhang, M.; Mao, B. W. *Chem. Commun.* **2012**, *48*, 582. (b) Zhang, X.; Zhong, Y.; Yan, J.; Mao, B. *J. Electrochem.* **2014**, *20*, 295.

(12) (a) Hoth, J.; Hausen, F.; Muser, M. H.; Bennewitz, R. *J. Phys.: Condens. Matter* **2014**, *26*, No. 284110. (b) Black, J. M.; Walters, D.; Labuda, A.; Feng, G.; Hillesheim, P. C.; Dai, S.; Cummings, P. T.; Kalinin, S. V.; Proksch, R.; Balke, N. *Nano Lett.* **2013**, *13*, 5954. (c) Labuda, A.; Grutter, P. *Langmuir* **2012**, *28*, 5319.

(13) (a) Perkin, S.; Crowhurst, L.; Niedermeyer, H.; Welton, T.; Smith, A. M.; Gosvami, N. N. *Chem. Commun.* **2011**, *47*, 6572. (b) Smith, A. M.; Lovelock, K. R. J.; Gosvami, N. N.; Licence, P.; Dolan, A.; Welton, T.; Perkin, S. *J. Phys. Chem. Lett.* **2013**, *4*, 378.

(14) (a) Ishino, T.; Hieda, H.; Tanaka, K.; Gemma, N. *Jpn. J. Appl. Phys., Part 2* **1994**, *33*, L1552. (b) Wang, J.; Bard, A. J. *J. Phys. Chem. B* **2001**, *105*, 5217.

(15) Hamm, U. W.; Kramer, D.; Zhai, R. S.; Kolb, D. M. *J. Electroanal. Chem.* **1996**, *414*, 85.

(16) Merlet, C.; Limmer, D. T.; Salanne, M.; van Roij, R.; Madden, P. A.; Chandler, D.; Rotenberg, B. *J. Phys. Chem. C* **2014**, *118*, 18291. Kornyshev, A. A.; Qiao, R. *J. Phys. Chem. C* **2014**, *118*, 18285.